ChemComm



COMMUNICATION

View Article Online



Cite this: Chem. Commun., 2024, 60, 14037

Received 15th October 2024, Accepted 30th October 2024

DOI: 10.1039/d4cc05463f

rsc.li/chemcomm

Synthesis of heteroleptic bis-phosphine bis-NHC iron (0) complexes: a strategy to enhance small molecule activation†

Christian M. Andre and Nathaniel K. Szymczak 10 *

We report the synthesis of heteroleptic iron complexes supported by both a bis-phosphine ligand (depe) and a bis-NHC ligand. The mixed ligand sets provide access to iron (0) adducts of N2 and CO that are highly activated, in comparison to homoleptic (i.e. Fe(depe)₂L) variants. Computational and experimental studies revealed the mixed ligand set distorts the geometric and electronic structure to yield an unusually basic iron. Although protonation occurred at Fe, silylation of the Fe(0)N2 complex afforded a highly activated silyldiazenido [FeNNSiMe₃]⁺ complex.

Low-valent iron complexes are routinely targeted as models for Fe-nitrogenase, given their ability to activate N2‡ as well as other small molecules (CO, CO₂, etc.), with iron phosphines among the most established (Fig. 1A).2 Of particular note is the Fe⁰N₂ complex of 1,2-bis(diethylphosphino)ethane (depe) because it features a significantly activated N2 ligand and is a catalyst for selective N₂ reduction to hydrazine.^{2a} These properties have motivated studies by our group3 and others4 to examine additional design principles, such as those achieved by introducing secondary sphere acids, to further enhance the activation imparted by the Fe⁰(depe)₂ unit to small molecules. While adjusting the primary coordination sphere of the iron centre to increase its electron density is the most common redesign strategy, modification of the phosphine from depe typically\(\) affords systems that are less donating than Fe(depe)₂⁵ and/or have a dramatically different steric profile and binding geometry. 2i,j,6 In analogy to phosphines, lower-coordinate iron complexes of monodentate N-heterocyclic carbenes (NHC) are reported to activate N2 to a greater extent (Fig. 1B), a result of their stronger σ -donor ability than phosphines.⁷

In contrast to the breadth of low-valent chemistry reported with phosphine donors, there are no such examples of

Department of Chemistry, University of Michigan, 930 North University Avenue, Ann Arbor, MI 48109, USA. E-mail: nszym@umich.edu

18-electron Fe⁰ complexes containing four NHC donors.⁸ To bridge the gap between Fe⁰ complexes containing four phosphines (known) and those containing four NHCs (unknown), we targeted systems containing two phosphines and two NHCs. Although mixed NHC/phosphine transition metal complexes9 have been reported, few examples contain bis-NHCs/bisphosphines, 9h-k and none involve iron. Assembling two distinct sets of bidentate ligands to form a heteroleptic complex is precedented for tuning a metal's reactivity and/or stability; 9,10 however, this approach has not been employed to improve N₂ activation.

Our design strategy employed a methylene-linked bis-NHC ligand, because it is a neutral bidentate ligand with similar steric profile and bite-angles to depe (Fig. 1C). 2d,11 We hypothesized that

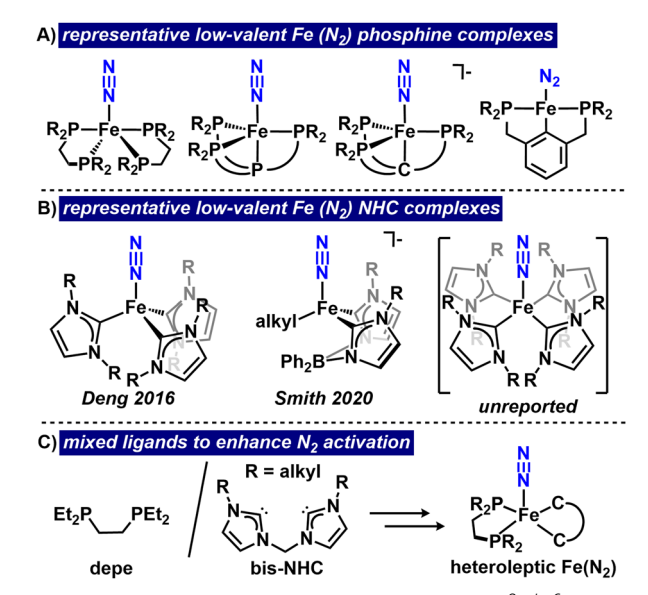
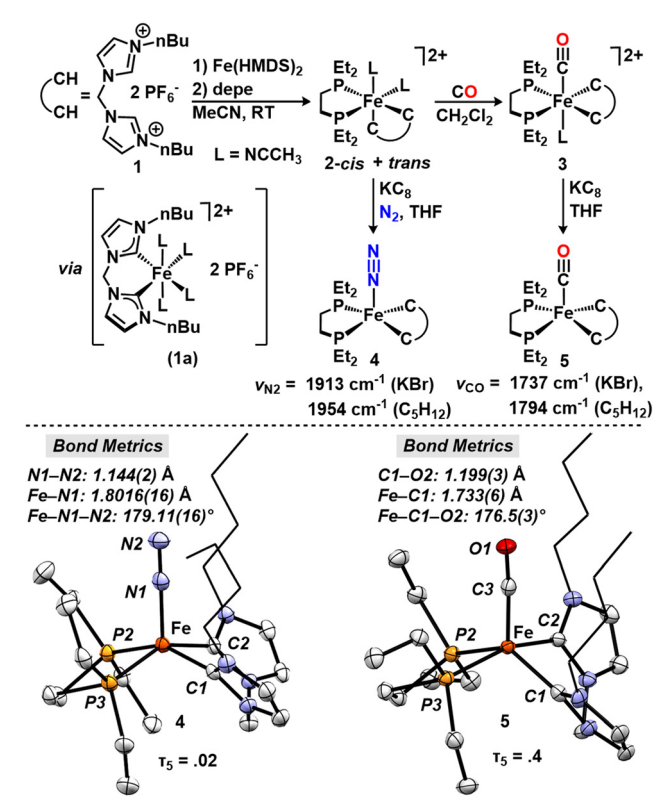


Fig. 1 (A) Fe phosphines demonstrated to activate N_2 . 2c,d,g,6a (B) Fe N_2 NHC complexes and the lack of a reported Fe N₂ tetracarbene. ^{7b,c} (C) Analogy between depe and bis-NHC ligand and the prospect of a heteroleptic complex

[†] Electronic supplementary information (ESI) available. CCDC 2368195, 2390974 and 2394085. For ESI and crystallographic data in CIF or other electronic format see DOI: https://doi.org/10.1039/d4cc05463f

Communication ChemComm



Scheme 1 Synthesis of heteroleptic complexes 2-5. Molecular structure of 4 determined by single crystal XRD. Thermal ellipsoids shown at 50% probability with hydrogen atoms omitted and non-interacting alkyl chains are in wireframe for clarity

a heteroleptic iron complex of both a bis-phosphine and a bis-NHC ligand would be structurally analogous to the established bis-(bis-phosphine) Fe⁰(depe)₂ system, but better able to promote substrate activation with a more electron-rich iron centre.

We developed a general one-pot metalation/ligand substitution procedure (Scheme 1), to access a mixed NHC/phosphine system. Introduction of 1 equiv. 1 (bis-N-butyl-imidazolium salt) to a suspension of Fe(N(SiMe₃)₂)₂ in CH₃CN afforded a clear red solution after 2 h at room temperature. Solvent removal by vacuum followed by washing with THF yielded a deep red solid. This red intermediate exhibited two aromatic ¹H NMR singlets at 7.46 and 7.32 ppm without further downfield resonances, consistent with a symmetrically bound bis-NHC tetrakis-MeCN complex (1a) analogous to a previous report. 12 To a CH₃CN solution of 1a was added 1.0 equiv. depe as a CH₃CN solution, which caused a colour change to deep orange. Concentration of this product under vacuum yielded a viscous solution, from which residual depe was removed via pentane extraction. Solvent removal yielded a bright orange diamagnetic complex 2 as a mixture of isomers in 95% yield.

ESI-mass spectrometry of 2 provided a m/z of 567.2671, consistent with $[Fe(HCOO)(^{butyl}CC)(depe)]^+$ $(m/z = 567.2674), \P$ which features a heteroleptic composition of the primary coordination sphere. The ¹H NMR spectrum in CH₂Cl₂ exhibited a set of four strong aromatic singlets (7.53, 7.38, 7.28, & 7.04 ppm) and a set of two weaker singlets (7.58 and 7.24 ppm) that integrate in a net ratio of $\sim 6:1$. The ³¹P NMR spectrum exhibited a pair of doublets (75.87 and 62.93 ppm, $J_{PP} = 15$ Hz) and a smaller singlet (62.56 ppm) that integrate to the same ratio (Fig. S2 and S3, ESI†). This pattern is consistent with a mixture of the cis-heteroleptic isomer (2-cis), where both phosphorus and NHC donors are inequivalent, and the trans heteroleptic isomer (2-trans), where they are equivalent. Following addition of MeCN- d_3 to 2, we observed a loss of coordinated MeCN ¹H NMR resonances (2.45 and 2.33 ppm) and growth of free MeCN (1.94 ppm). This behavior indicates facile exchange of MeCN ligands and may implicate a ligand exchange pathway for isomerization of 2. The structure of 2-cis was further confirmed by single crystal x-ray diffraction (SC-XRD) studies from crystals grown in CH₂Cl₂.

Although 2 was isolated as a mixture of cis and trans isomers, we found that addition of a neutral π -acid, such as CO, afforded a single geometric isomer. Charging a solution of 2 in CH₂Cl₂ with 30 psig CO caused the colour to slowly fade over 6 h. Evaporation of the solvent afforded a pale-yellow species (3). Its ³¹P NMR spectrum featured a singlet at 64.6 ppm, while the ¹H NMR spectrum exhibited aromatic resonances at 7.57 and 7.17 ppm that integrate 4:3 with a singlet at 2.48 ppm. This result is consistent with a trans geometry (C_s symmetry) containing a single acetonitrile ligand. ESI mass spectrometry of 3 provided a m/z of 295.6467, consistent with [Fe(CO)(MeCN) $(^{\text{butyl}}CC)(\text{depe})]^{2+}$ (m/z = 295.6451). IR spectroscopy of 3 revealed a single ν_{CO} stretch at 1947 cm⁻¹. These data support assignment of 3 as a heteroleptic complex containing a single carbonyl ligand trans to a coordinated CH₃CN. We attribute formation of the trans isomer of 3 to the strong trans donor properties of CO, which favours trans ligands that are weaker donors (MeCN), rather than stronger donors (NHC or phosphine), as would be necessitated by the *cis* isomer.

Following the synthesis of 2 and 3, we pursued an Fe⁰ species. Reduction of 2 with excess KC8 followed by pentane extraction/removal afforded a deep red diamagnetic solid (4). This species exhibits a sharp ³¹P NMR singlet at 90.05 ppm, and two aromatic ¹H singlets at 6.44 and 6.35 ppm. Subjecting 3 to analogous reduction conditions and workup yielded a diamagnetic orange solid (5). NMR spectra of 5 similarly exhibit a broad ³¹P NMR singlet at 95.85 ppm and two ¹H singlets at 6.45 and 6.32 ppm. The breadth of these NMR resonances of 4 and 5 vary with temperature (-75 °C to 45 °C), indicating fluxionality in solution.

Both 4 and 5 exhibited more activated π -acceptor ligands than their bis-depe Fe⁰ analogues: 4 displayed a strong ν_{N2} stretch at 1913 cm⁻¹ ($\nu_{N_2} = 1955 \text{ cm}^{-1} \text{ for FeN}_2(\text{depe})_2$) and 5 exhibited a strong v_{CO} stretch at 1737 cm⁻¹ (v_{CO} = 1800 cm⁻¹ for FeCO(depe)2). The ligand environment imposed on iron was assessed using cyclic voltammetry experiments. Compounds 4 and 5 exhibited reversible events at -2.48 V and -2.06 V (THF, vs. $Fe(Cp_2)/Fe(Cp)_2^+$, respectively, which we assign as Fe(0/1)redox couples. Relative to the bis-depe analogues, 4 and 5 are significantly more reducing (480 mV and 520 mV more cathodic, respectively2a, further supporting strongly reduced Fe centers.

ChemComm Communication

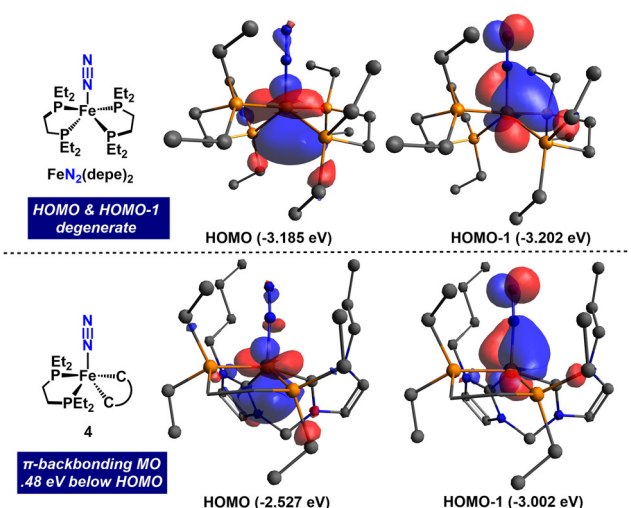


Fig. 2 Frontier orbitals from DFT performed at TPSS def2-TZVP level of theory with SMD solvation model on optimized structure (isosurface values = 0.05).

SC-XRD studies on 4 and 5 reveal structural differences from the analogous Fe(depe)₂ complexes. 5 exhibits an intermediate 5-coordinate (τ = 0.4) geometry and 4 has a square pyramidal $(\tau = 0.02)$ geometry, which contrast with the reported TBP geometry of $FeN_2(depe)_2$ and $FeCO(depe)_2$ ($\tau = 0.9$ for both). ^{7b,13} While the N-N bond distance of **4** is not statistically different from that of FeN₂(depe)₂, (1.144(2) Å vs. 1.139(13) Å), the C-O bond of 5 is longer than that of FeCO(depe)₂ (1.199(3) Å vs. 1.179(8) Å), consistent with its more activated IR stretch. Both the Fe-N₂ bond of 4 and the Fe-CO bond of 5 are longer than their Fe(depe)₂ analogues (1.8016(16) Å vs. 1.748(8) Å for FeN₂; 1.733(6) Å vs. 1.179(8) Å for FeCO), which reflects less multiple bond character between iron and the bound diatoms, despite greater π -backdonation (Scheme 1).

Geometry optimization of both 4 and 5 using density functional theory (DFT) converged to intermediate structures ($\tau = 0.4$). IR spectra and Fe(0/1) redox potentials for both FeN₂(depe)₂ and 4 calculated from these DFT optimization studies corroborate solution-phase experimental results (Table S4, ESI†), supporting the intermediate geometry as the solution-phase structure of 4. This optimized structure also reveals an elongated N-N bond in 4 with respect to FeN₂(depe)₂ (1.142 Å vs. 1.139 Å), indicating increased activation of the N_2 ligand. Molecular orbital (MO) calculations for 4 and FeN₂(depe)₂ illustrate energetic differences between the frontier orbitals (Fig. 2). The HOMO of 4 is localized on the Fe centre, is σ -antibonding with respect to N₂ coordination, and higher in energy than that of FeN₂(depe)₂, which validates elongated Fe-N2 and Fe-CO bonds found in crystal structures of 4 and 5.

The HOMO-1 of 4 is the primary orbital involved in π -backdonation into the N₂ π * orbital; however it is -0.475 eV lower than the HOMO. Despite the HOMO-1 being higher in energy in 4 than in FeN₂(depe)₂, this orbital sits far below the metal-centred HOMO. This electronic structure renders the complex more basic at Fe, and less likely to protonate at N₂ than for FeN₂(depe)₂. We attribute the higher orbital energies of 4 to the greater donor strength of the NHC ligands, while the distortion of its geometric and electronic structure is due to the inherent asymmetry of the heteroleptic ligand environment.

To augment the DFT studies that predict high Fe-basicity of 4, we studied its reactivity with Brønsted acids. Treating 4 with [NH₂Ph₂][OTf] in THF afforded a rapid color change from red to yellow. This product exhibits a triplet ¹H NMR resonance spectrum at -16.7 ppm (${}^2J_{HP} = 60$ Hz), a doublet ${}^{31}P$ NMR resonance at 81.9 ppm (${}^{2}J_{HP}$ = 59 Hz), and an IR absorbance at 2072 cm⁻¹. These data are consistent with prior reports of $[FeH(N_2)]^+$ complexes, 2a,k as protonation of $FeN_2(depe)_2$ with 1 equiv. [NH₂Ph₂][OTf] afforded trans-[Fe(H)N₂(depe)₂]⁺, characterized by a 1 H NMR quintet at -18.20 ppm, a 31 P doublet at 81.14 ppm (${}^2J_{HP}$ = 50 Hz), and an IR feature at 2090 cm⁻¹ (ν_{N2}). Therefore we assign this product as trans-[FeH(N2)(depe) (butylCC) [OTf] ([6][OTf]) (Fig. 3). Treatment of 4 with a weaker acid, ^tBuOH, affords 6 quantitatively by NMR spectroscopy, but subjecting FeN₂(depe)₂ to the same conditions yields <15% protonation. This divergence in reactivity demonstrates the higher basicity of the Fe center predicted by DFT in 4 compared to FeN2(depe)2.

To minimize Fe-centered reactivity, we targeted a more sterically encumbered electrophile, trimethylsilyl triflate (SiMe₃OTf), for N₂ functionalization, analogous to reported silylation of FeN2(depe)2.14 Addition of 1 eq of SiMe3OTf to an Et₂O solution of 4 at -78 °C afforded a deep green precipitate (7) in 75% yield (Fig. 3). This species exhibits a ³¹P NMR singlet at 85.3 ppm, and two aromatic 1H singlets at 7.68 and 7.16 ppm, which is consistent with a Fe^{II} heteroleptic complex. These aromatic features integrated net 4:9 with respect to a ¹H singlet at 0.19 ppm, consistent with incorporation of one SiMe₃ group. A single ¹⁹F NMR resonance at -78.9 ppm is consistent with a free triflate anion in the product, indicating a cationic iron complex. 29Si NMR spectroscopy revealed a singlet at -5.4 ppm, and ATR-IR characterization of 7 exhibited a strong absorbance at 1693 cm⁻¹; both of which are consistent with a silyldiazenide ("NNSiMe₃) substituent. These spectra are similar to those of the reported $[Fe(N_2SiMe_3)(depe)_2]^+$ $(N_2SiMe_3 unit =$ ¹H NMR: 0.20 ppm, ²⁹Si NMR: 6.4 ppm, IR: 1732 cm⁻¹). ¹⁴ In contrast to the reaction of FeN2(depe)2 with SiMe3OTf, which was reported to be reversible, 7 formed cleanly and irreversibly, supporting the increased basicity of the N₂ moiety of 4. Compared to other reported iron silyldiazenido complexes, of which most are neutral, 1b,15 the IR absorbance suggests that 7 is among the most activated, only surpassed by an anionic example^{1b} from the Holland group, despite assignment of 7

$$\begin{array}{c} \text{Me}_3\text{Si} \\ \text{N} \\ \text{Pr} \\ \text{Pr} \\ \text{Et}_2 \\ \text{V} \\ \text{Pr} \\ \text{Et}_2 \\ \text{V} \\ \text{Pr} \\ \text{Fe} \\ \text{C} \\ \text{Et}_2 \\ \text{V} \\ \text{Fe} \\ \text{Et}_2 \\ \text{V} \\ \text{Fe} \\ \text{C} \\ \text{Et}_2 \\ \text{V} \\ \text{Fe} \\ \text{Fe} \\ \text{C} \\ \text{Et}_2 \\ \text{V} \\ \text{Fe} \\ \text{Fe} \\ \text{C} \\ \text{Fe} \\ \text{Et}_2 \\ \text{V} \\ \text{Fe} \\ \text{Fe} \\ \text{Fe} \\ \text{C} \\ \text{Fe} \\ \text{Fe} \\ \text{C} \\ \text{Fe} \\ \text{$$

Fig. 3 Synthesis of 6 and 7 from 4.

Communication

as cationic. While the heteroleptic iron system and Fe(depe)₂ demonstrate similar aptitude for N2 silylation, each heteroleptic intermediate (the N2 (4) and silylhydrazide (7) complexes) exhibit substantially more activated N-N bonds at each step.

In conclusion, we have reported the synthesis and characterization of a new class of heteroleptic Fe⁰ complexes jointly supported by a bis-phosphine and a methylene-linked bis-NHC ligand. The dinitrogen and carbonyl complexes, 4 and 5, are highly reduced, as exemplified by their highly activated $\nu_{\rm N2}/\nu_{\rm CO}$ stretches and cathodic redox potentials. SC-XRD and DFT studies reveal that both 4 and 5 adopt an intermediate 5 coordinate geometry ($\tau = 0.4$). Silylation of 4 yields a highly activated silydiazenido complex 7, demonstrating the system's potential for N₂ functionalization. This mixed-ligand Fe⁰ system exhibits properties uncharacteristic of reported Fe⁰ phosphine or NHC complexes, and the modular access to heteroleptic Fe⁰N₂ compounds presented herein invites further work to tune the primary sphere donors and induce new reactivity at iron.

C. A. performed the experiments. N.K.S managed the project. Both C. A. and N. K. S. designed and analysed experiments and wrote the manuscript.

This work was supported by the NIH (R35GM136360). We thank Fengrui Qu for SCXRD collection of 2-cis, 4, and 5 and the Buss Lab for assistance with inert atmosphere IR spectroscopy.

Data availability

The data supporting this article have been included as part of the ESI.† Crystallographic data for 2-cis, 4, and 5 have been deposited at the CCDC under and can be obtained from https:// www.ccdc.cam.ac.uk/structures.

Conflicts of interest

There are no conflicts to declare.

Notes and references

- ‡ For N2, we use the term "activation" to refer to a lower N-N bond order, assessed structurally, or by IR spectroscopy ($\nu_{\rm N2}$).¹⁶
- § A notable exception is the ligand DMeOPrPE.
- ¶ Formate (HCOO⁻) is present in the ESI-MS eluent solution.
- 1 (a) J. S. Anderson, J. Rittle and J. C. Peters, Nature, 2013, 501, 84; (b) S. F. McWilliams, D. L. J. Broere, C. J. V. Halliday, S. M. Bhutto, B. Q. Mercado and P. L. Holland, Nature, 2020, 584, 221; (c) M. M. Rodriguez, E. Bill, W. W. Brennessel and P. L. Holland, Science, 2011, 334, 780-783; (d) S. Kuriyama, K. Arashiba, K. Nakajima, Y. Matsuo, H. Tanaka, K. Ishii, K. Yoshizawa and Y. Nishibayashi, Nat. Commun., 2016, 7, 12181; (e) S. M. Rummelt, H. Zhong, I. Korobkov and P. J. Chirik, J. Am. Chem. Soc., 2018, 140, 11589.
- 2 (a) P. J. Hill, L. R. Doyle, A. D. Crawford, W. K. Myers and A. E. Ashley, J. Am. Chem. Soc., 2016, 138, 13521; (b) M. M. Deegan and J. C. Peters, J. Am. Chem. Soc., 2017, 139, 2561; (c) S. Kuriyama, T. Kato, H. Tanaka, A. Konomi, K. Yoshizawa and Y. Nishibayashi, Bull. Chem. Soc. Jpn., 2022, 95, 683; (d) M. Hirano, M. Akita, T. Morikita, H. Kubo, A. Fukuoka and S. Komiya, Dalton Trans., 1997, 3453; (e) M. V. Baker and L. D. Field, Organometallics, 1986, 5, 821; (f) H. H. Karsch, Chem. Ber., 1977, 110, 2213; (g) S. E. Creutz

- and J. C. Peters, J. Am. Chem. Soc., 2014, 136, 1105; (h) T. T. Adamson, S. P. Kelley and W. H. Bernskoetter, Organometallics, 2020, 39, 3562; (i) D. J. Schild and J. C. Peters, ACS Catal., 2019, 9, 4286; (j) T. A. Betley and J. C. Peters, J. Am. Chem. Soc., 2004, 126, 6252; (k) L. D. Field, N. Hazari and H. L. Li, *Inorg. Chem.*, 2015, 54, 4768; (1) G. J. Leigh and M. Jimenez-Tenorio, J. Am. Chem. Soc., 1991, 113, 5862; (m) A. Hills, D. L. Hughes, M. Jimenez-Tenorio, G. J. Leigh and A. T. Rowley, Dalton Trans., 1993, 3041.
- 3 J. B. Geri, J. P. Shanahan and N. K. Szymczak, J. Am. Chem. Soc., 2017, **139**, 5952.
- 4 (a) H. Corona, M. Pérez-Jiménez, F. de la Cruz-Martínez, Fernández and J. Campos, Angew. Chem., Int. Ed., 2022, 61, e202207581; (b) A. D. Piascik, R. Li, H. J. Wilkinson, J. C. Green and A. E. Ashley, J. Am. Chem. Soc., 2018, 140, 10691.
- 5 (a) R. A. Cable, M. Green, R. E. Mackenzie, P. L. Timms and T. W. Turney, J. Chem. Soc. Chem. Commun., 1976, 7, 270; (b) A. M. Tondreau, B. L. Scott and J. M. Boncella, Organometallics, 2016, 35, 1643; (c) J. D. Gilbertson, N. K. Szymczak and D. R. Tyler, J. Am. Chem. Soc., 2005, 127, 10184.
- 6 (a) R. Gilbert-Wilson, L. D. Field, S. B. Colbran and M. M. Bhadbhade, Inorg. Chem., 2013, 52(6), 3043-3053; (b) L. D. Field, H. L. Li, S. J. Dalgarno and R. D. McIntosh, Eur. J. Inorg. Chem., 2019, 2006–2011; (c) F. F. van de Watering, W. Stroek, J. Ivar van der Vlugt, B. de Bruin, W. I. Dzik and J. N. H. Reek, Eur. J. Inorg. Chem., 2018, 1254-1265; (d) D. E. Prokopchuk, E. S. Wiedner, E. D. Walter and C. V. Popescu, et al., J. Am. Chem. Soc., 2017, 139(27), 9291-9301; (e) A. Cavaillé, B. Joyeux, N. Saffon-Merceron, N. Nebra, M. Fustier-Boutignon and N. Mézailles, Chem. Commun., 2018, 54(84), 11953.
- 7 (a) Y. Fan, J. Cheng, Y. Gao, M. Shi and L. Deng, Chem. Sin., 2018, 76, 445; (b) Z. Ouyang, J. Cheng, L. Li, X. Bao and L. Deng, Chem. - Eur. J., 2016, 22, 14162; (c) S. A. Lutz, A. K. Hickey, Y. Gao, C.-H. Chen and J. M. Smith, J. Am. Chem. Soc., 2020, 142, 15527.
- 8 C. R. Groom, M. P. Lightfoot and S. C. Ward, Acta Crystallogr., 2016, B72, 171.
- 9 (a) A. Ahmida, F. M. Elmagbari, H. Egold, U. Flörke and G. Henkel, Polyhedron, 2020, 181, 114472; (b) A. Ahmida, F. M. Elmagbari, H. Egold and G. Henkel, Polyhedron, 2021, 198, 115083; (c) P. Ai, A. A. Danopoulos and P. Braunstein, Dalton Trans., 2016, 45, 4771; (d) B. R. Galan, E. S. Wiedner, M. L. Helm, J. C. Linehan and A. M. Appel, Organometallics, 2014, 33, 2287; (e) P. Nagele, U. Herrlich, F. Rominger and P. Hofmann, Organometallics, 2013, 32, 181; (f) E. Mosaferi, L. Pan, T. Wang, Y. Sun, C. Pranckevicius and D. W. Stephan, *Dalton Trans.*, 2016, 45(4), 1354; (g) N. Stylianides, N. Tsoreas and A. A. Daopoulos, J. Organomet. Chem., 2005, 690, 5948; (h) X. Liu and W. Chen, Dalton Trans., 2011, 41(2), 599; (i) O. Bárta, P. Pinter, I. Císařová, T. Strassner and P. Štěpnička, Eur. J. Inorg. Chem., 2020, 575-580; (j) A. L. Ostericher, K. M. Waldie and C. P. Kubiak, ACS Catal., 2018, 8(10), 9596; (k) M. V. Baker, S. K. Brayshaw, B. W. Skelton, A. H. White and C. C. Williams, J. Organomet. Chem., 2005, 690(9), 2312.
- 10 (a) S. Gonell, E. A. Assaf, J. Lloret-Fillol and A. J. M. Miller, ACS Catal., 2021, 11(24), 15212; (b) Y. Liu, K. S. Kjær, L. A. Fredin, P. Chábera and T. Harlang, et al., Chem. - Eur. J., 2015, 21(9), 3628; (c) K. Witas, S. S. Nair, T. Maisuradze, L. Zedler, H. Schmidt and P. Garcia-Porta, et al., J. Am. Chem. Soc., 2024, 146(29), 19710.
- 11 S. Meyer, C. M. Orben, S. Demeshko, S. Dechert and F. Meyer, Organometallics, 2011, 30(24), 6692.
- 12 J. Rieb, A. Raba, S. Haslinger, M. Kaspar, A. Pöthig, M. Cokoja, J.-M. Basset and F. E. Kühn, Inorg. Chem., 2014, 53, 9598.
- 13 S. Komiya, M. Akita, A. Yoza, N. Kasuga, A. Fukuoka and Y. Kai, J. Chem. Soc. Chem. Commun., 1993, 9, 787.
- 14 A. D. Piascik, P. J. Hill, A. D. Crawford, L. R. Doyle, J. C. Green and A. E. Ashley, Chem. Commun., 2017, 53, 7657.
- 15 (a) Y. Ohki, K. Munakata, Y. Matsuoka, R. Hara, M. Kachi, K. Uchida, M. Tada, R. E. Cramer, W. M. C. Sameera and T. Takayama, et al., Nature, 2022, 607, 86-90; (b) M.-E. Moret and J. C. Peters, J. Am. Chem. Soc., 2011, 133, 18118; (c) Y. Lee, N. P. Mankad and J. C. Peters, Nat. Chem., 2010, 2, 558; (d) J. Rittle and J. C. Peters, Proc. Natl. Acad. Sci. U. S. A., 2013, **110**, 15898.
- 16 J. L. Crossland and D. R. Tyler, Coord. Chem. Rev., 2010, 254, 1883.